JOURNAL OF GUIDANCE, CONTROL, AND DYNAMICS
Vol. 21, No. 2, March–April 1998

Simultaneous Deployment of a Cable from Two Moving Platforms

S. Djerassi* and H. Bamberger†
RAFAEL, Ministry of Defense, Haifa 31021, Israel

The deployment of a cable from two moving platforms is examined. The cable is regarded as a collection of links whose number increases with time. An order-*n* algorithm is constructed for the simulation of the motion of the cable during deployment, incorporating a novel, three-pass procedure for the identification of constraint forces appearing in the equations of motion and a procedure for the release of the cable from both platforms. The algorithm is described, and the use of the associated simulation program is illustrated by means of an example.

Introduction and Model Description

CABLE-CONNECTED vehicles are of increasing interest in space, marine, and airborne applications. Analyses of tethered satellites,[1–5] cable-controlled submarines,[6,7] and towed airborne vehicles[8,9] demonstrate this interest. One version of the cable deployment problem refers to a system S consisting of two moving platforms P and C, releasing a cable from points $\bar{P}$ and $\hat{C}$ of containers V_P and V_C fixed to P and C, respectively, as shown in Fig. 1. Such a model is of interest, for example, in connection with systems described in Refs. 10–12. The cable in these references comprises an optical fiber deployed passively, i.e., without active control of tension or of deployment rate. Now, cables are usually deployed from one platform, even if they connect two platforms.[1,6] However, if an optical fiber is released from one platform, say P in Fig. 1, then motions of the second platform C, e.g., away from P, may induce a high tensile force on the fiber due to aerodynamic drag. Premature failure of even a relatively short fiber (a few kilometers) is likely to occur. Deployment from both platforms keeps the cable essentially floating, so that the tension remains within acceptable limits.

Two basic approaches are used in Refs. 1–9 to model cables analytically. One approach regards the cable as a continuum and describes elastic deformation with the aid of modal functions.[1–4] A second approach regards the cable as consisting of relatively short links arranged in a chain topology, connected to each other by means of revolute joints,[5–9] and elastic deformations are described as relative rotations of the links with respect to one another. References 1, 3, and 4, using the first approach, and Refs. 5 and 6, using the second approach, consider deployment or retraction of a cable from one platform, whereas Refs. 2 and 7–9 deal with constant-length cables.

A method suitable for the simulation of motions of systems deploying a cable from two platforms has to allow the cable to assume an arbitrary configuration, e.g., loop shape or shapes involving local, small radii of curvature. The continuum approach falls short of this requirement, as only cable configurations deviating slightly from the respective undeformed configurations are allowed. This is also the case if the approach of Ref. 4 is taken. There, a cable is assumed to consist of a relatively small, predetermined number of sections of variable length, each regarded as elastic, and is treated as in Refs. 1 and 3. Furthermore, the method used in Refs. 1 and 3 to accommodate changes in the cable length is based on a change in the modal functions. In the present context (passive deployment), this method does not enable the determination of the length of the cable deployed from each of the platforms.

Thus, one has to resort to the second approach, where cables are regarded as dynamical systems with a chain topology. Such a model was dealt with by numerous researchers. Taking advantage of the special properties of systems consisting of chain connected bodies, these researchers established specific formulations for the generation of equations governing the motions of such systems.[13,14] Furthermore, the fact that recursive algorithms can be applied to such a topology attracted attention, ultimately leading to the development of extremely efficient algorithms, often called order-n algorithms. (The number of operations required by these algorithms in the context of numerical solutions of the associated equations is proportional to n, the number of degrees of freedom. By way of contrast, the number of operations required by algorithms associated with an arbitrary topology is proportional to n^3.) For instance, Rosenthal's order-n algorithm for a chain topology multibody system[15] was used by Banerjee[5] to simulate motions of a cable (or a beam) deployed from or retracted into a platform having a prescribed motion, so that n becomes a function of time. Revisions are required in this algorithm if the motion of the endpoint of the cable is prescribed, as when the cable is connected to a second moving platform. The force exerted by the latter on the cable endpoint must be determined before the motion variables can be evaluated. This state of affairs is dealt with in Ref. 6. Constraint equations containing nonlinear functions of measure numbers of the indicated force are formed (these nonlinearities result from the control forces governing the deployment/retraction) and solved iteratively for the latter. The number of links is assumed to be constant; however, the length of the links is time dependent, enabling deployment (or retraction). Again, this approach is not suitable when deployment proceeds from two platforms, as it is impossible to determine the length of the cable deployed from each of the platforms.

This paper presents a new method that deals with each of the issues just mentioned. First, the model in Fig. 1 is described in detail. The masses of the platforms are assumed to significantly exceed that of the cable, so that their motion is not affected by the deployment process. Furthermore, $\bar{P}$ and $\hat{C}$ are regarded as moving along predetermined trajectories TP and TC, respectively, with known velocities $\boldsymbol{v}^{\bar{P}}$ and $\boldsymbol{v}^{\hat{C}}$. The cable is represented by a chain of $N(t)$ rigid links $C_{N1}, \ldots, C_{N2}$, where $N1(t)$ and $N2(t)$ are the numbers of the first active link and the last active link, so that $N(t) = N2(t) - N1(t) + 1$. The endpoints of C_n, the nth link, are denoted $\bar{P}_n$ and P_n, and C_n is assumed to be of length L_n and of mass ρL_n lumped at $P_n (n = N1, \ldots, N2)$. Point $\bar{P}_n$ is connected to point P_{n-1} by means of two revolute joints. Accordingly, the configuration of the cable is determined by $q_{N1}, \ldots, q_{N2}$ and $\bar{q}_{N1}, \ldots, \bar{q}_{N2}$, $2N$ angles describing the orientation of $C_{N1}, \ldots, C_{N2}$ in $\mathfrak{n}$, a Newtonian reference frame, as shown in Fig. 2a for C_n. In addition, S is subject to the following configuration constraints, namely, that P_{N2} moves along TP, whereas $\bar{P}_{N1}$ is attached to $\hat{C}$ at all times.

The motion of the cable is described with the aid of $\dot{q}_{N1}, \ldots, \dot{q}_{N2}$ and $\dot{\bar{q}}_{N1}, \ldots, \dot{\bar{q}}_{N2}$ and is subject to motion constraints associated with the indicated configuration constraints. These are

Received Aug. 23, 1996; presented as Paper 97-139 at the AAS/AIAA Space Flight Mechanics Conference, Huntsville, AL, Feb. 10–12, 1997; revision received July 25, 1997; accepted for publication July 26, 1997.

*Chief R&D Engineer, P.O. Box 2250.
†Research Engineer, P.O. Box 2250.

$$\boldsymbol{v}^{P_{N2}} \cdot \boldsymbol{n}_{pi} = 0 \qquad (i = 1, 2) \tag{1}$$

$$\boldsymbol{v}^{\bar{P}_{N1}} = \boldsymbol{v}^{\hat{C}} \tag{2}$$

where $\boldsymbol{v}^{P_{N2}}$ and $\boldsymbol{v}^{\bar{P}_{N1}}$ are the velocities of P_{N2} and $\bar{P}_{N1}$ in $\mathfrak{n}$, and $\boldsymbol{n}_{pi}$ $(i = 1, 2)$ are two unit vectors perpendicular to TP. These, together with $\boldsymbol{n}_t$, a unit vector tangent to TP at P_{N2}, form a set of dextral, mutually perpendicular unit vectors fixed to TP at P_{N2}. The orientation of this set in $\mathfrak{n}$ is determined by θ and φ, two angles described in Fig. 2b. Furthermore, it is assumed that P_{N2} is acted upon by a force $\boldsymbol{T}$ given by

$$\boldsymbol{T} = \rho v^2 \boldsymbol{n}_t \tag{3}$$

where v is defined as $v \triangleq (\boldsymbol{v}^{\bar{P}} - \boldsymbol{v}^{P_{N2}}) \cdot \boldsymbol{n}_t$. Finally, the cable is released passively from $\bar{P}$ as $\bar{P}$ moves along TP, whereas release of the cable from $\hat{C}$ occurs when the tension in the cable at $\bar{P}_{N1}$ exceeds a predetermined value $\bar{T}$. Thus, V_C serves as a safety valve, ensuring that the tension at $\bar{P}_{N1}$ does not exceed $\bar{T}$. As will be shown, this model can be used to investigate a variety of deployment problems, for example, the dependence of the cable tension on external winds or currents, the design of platform trajectories that prevent interference with the cable, or the determination of $\bar{T}$ and of the length of the cable being deployed from $\bar{P}$ and from $\hat{C}$ in a given mission.

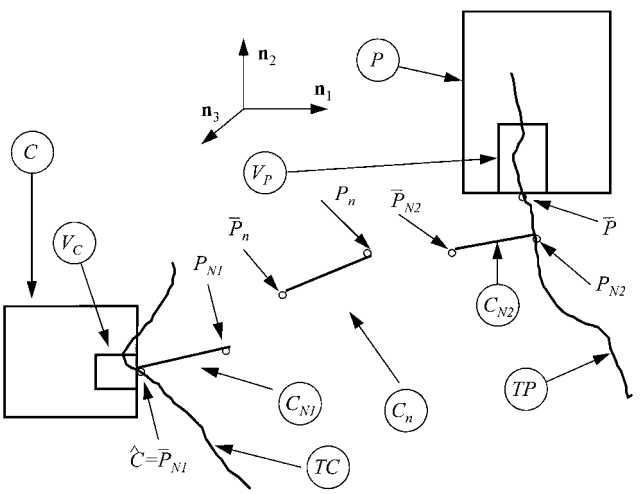

Fig. 1 Model.

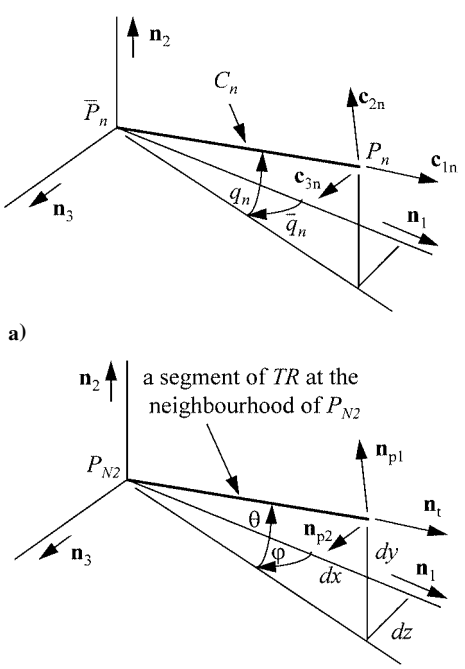

Fig. 2 Configurations of C_n and TP at P_{N2}.

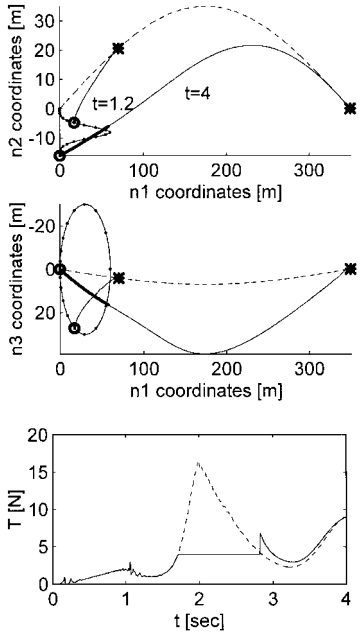

Fig. 3 Snapshots of cable configurations.

Fig. 4 Cable tension at $\hat{C}$.

It is the purpose of this paper to construct equations governing motions of the cable throughout the deployment process and to obtain descriptions such as the one in Fig. 3, showing snapshots of the cable during a typical deployment, and that in Fig. 4, showing the associated tension at $\hat{C}$. A novel, recursive, three-pass, order-n algorithm is constructed, dealing with equation generation, constraint forces evaluation, constraints satisfaction, and links release. The algorithm is described in detail in the next section, and its use is illustrated by means of an example, resulting in Figs. 3 and 4. A discussion of additional features of the new algorithm concludes this work.

Algorithm

A. Recursive, Three-Pass Algorithm

Let $\boldsymbol{c}_{in}$ $(i = 1, 2, 3)$ and $\boldsymbol{n}_i$ $(i = 1, 2, 3)$ be two sets of three dextral, mutually perpendicular unit vectors fixed in C_n and in $\mathfrak{n}$, respectively, and let $\boldsymbol{c}_{in}$ be initially aligned with $\boldsymbol{n}_i$ $(i = 1, 2, 3)$. Then C_n is brought to the orientation shown in Fig. 2a as follows: C_n is subject to an $\boldsymbol{n}_2$ rotation of amount $-\bar{q}_n$ and then to a $\boldsymbol{c}_{3n}$ rotation of amount q_n. The velocity $\boldsymbol{v}^{P_n}$ of P_n is given by

$$\boldsymbol{v}^{P_n} = \boldsymbol{v}^{P_{n-1}} + L_n \dot{q}_n \boldsymbol{c}_{2n} + L_n c_n \dot{\bar{q}}_n \boldsymbol{c}_{3n} \qquad (n = N1, \ldots, N2) \tag{4}$$

where $\boldsymbol{v}^{P_{n-1}}$ is the velocity of P_{n-1}; $s_n \triangleq \sin q_n$, $c_n \triangleq \cos q_n$, and $t_n \triangleq \tan q_n$; and it is implied that, for $n = N1$, $\boldsymbol{v}^{P_{N1-1}} = \boldsymbol{v}^{\bar{P}_{N1}} = \boldsymbol{v}^{\hat{C}}$ [Eq. (2)]. Hence,

$$\boldsymbol{a}^{P_n} = \boldsymbol{a}^{P_{n-1}} - L_n\left(\dot{q}_n^2 + c_n^2 \dot{\bar{q}}_n^2\right)\boldsymbol{c}_{1n} + L_n\left(\ddot{q}_n + s_n c_n \dot{\bar{q}}_n^2\right)\boldsymbol{c}_{2n}$$

$$- L_n\left(2 s_n \dot{q}_n \dot{\bar{q}}_n - c_n \ddot{\bar{q}}_n\right)\boldsymbol{c}_{3n} \qquad (n = N1, \ldots, N2) \tag{5}$$

and

$$a_i^{P_n} \triangleq \boldsymbol{a}^{P_n} \cdot \boldsymbol{n}_i \qquad (i = 1, 2, 3; \quad n = N1, \ldots, N2) \tag{6}$$

where $\boldsymbol{a}^{P_n}$ is the acceleration of P_n in $\mathfrak{n}$, $a_i^{P_n}$ $(i = 1, 2, 3;\ n = N1, \ldots, N2)$ are the respective measure numbers, and where it is implied that $\boldsymbol{a}^{P_{N1-1}} = \boldsymbol{a}^{\bar{P}_{N1}} = \boldsymbol{a}^{\hat{C}}$. Moreover, if A_{n-1}, $A_{n-1}^{(2)}$, and $A_{n-1}^{(3)}$ denote the $-\boldsymbol{n}_1$, $-\boldsymbol{n}_2$, and $-\boldsymbol{n}_3$ measure numbers of the resultant of forces exerted on $\bar{P}_n$ by P_{n-1}, and if the torques of couples (associated with elastic and damping properties of the cable) exerted by C_{n-1} and C_{n+1} on C_n are neglected, then

$$A_{n-1}^{(2)} = \frac{A_{n-1} t_n}{\bar{c}_n} \tag{7}$$

$$A_{n-1}^{(3)} = A_{n-1} \bar{t}_n \tag{8}$$

where $\bar{s}_n \triangleq \sin \bar{q}_n$, $\bar{c}_n \triangleq \cos \bar{q}_n$, and $\bar{t}_n \triangleq \tan \bar{q}_n$. These equations are obtained if the sum of the moments about P_n of all the forces acting on C_n is set equal to zero. Similarly, A_n, $A_n t_{n+1}/\bar{c}_{n+1}$, and $A_n \bar{t}_{n+1}$ are the measure numbers in the $\boldsymbol{n}_1$, $\boldsymbol{n}_2$, and $\boldsymbol{n}_3$ directions of the force

exerted on P_n by $\bar{P}_{n+1}$. Last, $\boldsymbol{D}^{P_n}$, the resultant of gravity forces, aerodynamical forces, hydrodynamical forces, etc., assumed to be exerted on C_n at P_n, can be expressed as

$$\boldsymbol{D}^{P_n} = D_1^{P_n}\boldsymbol{n}_1 + D_2^{P_n}\boldsymbol{n}_2 + D_3^{P_n}\boldsymbol{n}_3 \qquad (n = N1, \ldots, N2) \quad (9)$$

where $D_i^{P_n}$ $(i = 1, 2, 3)$ are the respective measure numbers. With k_{1n}, k_{2n}, and k_{3n} defined as

$$k_{1n} \hat{=} -A_{n-1} - \rho L_n\left[a_1^{P_{n-1}} - L_n c_n \bar{c}_n\left(\dot{q}_n^2 + \dot{\bar{q}}_n^2\right) + 2L_n s_n \bar{s}_n \dot{q}_n \dot{\bar{q}}_n\right] + D_1^{P_n} \qquad (n = N1, \ldots, N2) \quad (10)$$

$$k_{2n} \hat{=} -A_{n-1}t_n/\bar{c}_n - \rho L_n\left(a_2^{P_{n-1}} - L_n s_n \dot{q}_n^2\right) + D_2^{P_n} \qquad (n = N1, \ldots, N2) \quad (11)$$

$$k_{3n} \hat{=} -A_{n-1}\bar{t}_n - \rho L_n\left[a_3^{P_{n-1}} - L_n c_n \bar{s}_n\left(\dot{q}_n^2 + \dot{\bar{q}}_n^2\right) - 2L_n s_n \bar{c}_n \dot{q}_n \dot{\bar{q}}_n\right] + D_3^{P_n} \qquad (n = N1, \ldots, N2) \quad (12)$$

the equations governing the motion of C_n in $\mathfrak{n}$ are

$$k_{1n} + A_n + \rho L_n^2(s_n \bar{c}_n \ddot{q}_n + \bar{s}_n c_n \ddot{\bar{q}}_n) = 0 \qquad (n = N1, \ldots, N2 - 1) \quad (13)$$

$$k_{2n} + A_n t_{n+1}/\bar{c}_{n+1} - \rho L_n^2 c_n \ddot{q}_n = 0 \qquad (n = N1, \ldots, N2 - 1) \quad (14)$$

$$k_{3n} + A_n \bar{t}_{n+1} + \rho L_n^2(s_n \bar{s}_n \ddot{q}_n - c_n \bar{c}_n \ddot{\bar{q}}_n) = 0 \qquad (n = N1, \ldots, N2 - 1) \quad (15)$$

obtained with the aid of Fig. 5. These can be solved for A_n, $\ddot{q}_n$, and $\ddot{\bar{q}}_n$, yielding

$$A_n = -\frac{(k_{1n}\bar{c}_n + k_{2n}t_n + k_{3n}\bar{s}_n)c_n}{c_n\bar{c}_n + t_{n+1}s_n/\bar{c}_{n+1} + \bar{s}_n c_n \bar{t}_{n+1}} \qquad (n = N1, \ldots, N2 - 1) \quad (16)$$

$$\ddot{q}_n = \frac{k_{2n} + A_n t_{n+1}/\bar{c}_{n+1}}{\rho L_n^2 c_n} \qquad (n = N1, \ldots, N2 - 1) \quad (17)$$

$$\ddot{\bar{q}}_n = \frac{k_{3n} + A_n \bar{t}_{n+1} + \rho L_n^2 s_n \bar{s}_n \ddot{q}_n}{\rho L_n^2 c_n \bar{c}_n} \qquad (n = N1, \ldots, N2 - 1) \quad (18)$$

Now, Eqs. (16–18) are not valid for $n = N2$ (q_{N2+1} and $\bar{q}_{N2+1}$ do not exist). Moreover, P_{N2} is acted upon by a known force $\boldsymbol{T}$ [see Eq. (3)] and, in addition, by an unknown force exerted by TP on P_{N2}, whose measure numbers in the $\boldsymbol{n}_{p1}$ and $\boldsymbol{n}_{p2}$ directions are denoted F_1 and F_2. Hence, for $n = N2$, Eqs. (13–15) are replaced with

$$k_{1N2} + \rho L_{N2}^2(s_{N2}\bar{c}_{N2}\ddot{q}_{N2} + \bar{s}_{N2}c_{N2}\ddot{\bar{q}}_{N2}) + \rho v^2 c\varphi c\theta - F_1 s\theta c\varphi - F_2 s\varphi = 0 \quad (19)$$

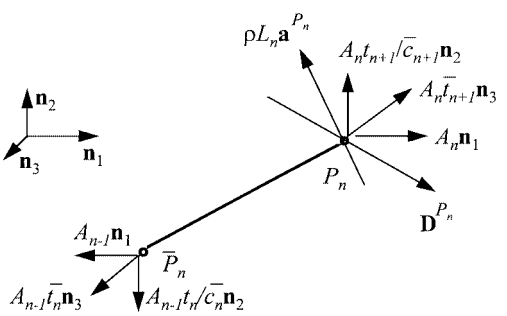

Fig. 5 Free body diagram of the *n*th link.

$$k_{2N2} - \rho L_{N2}^2 c_{N2}\ddot{q}_{N2} + \rho v^2 s\theta + F_1 c\theta = 0 \quad (20)$$

$$k_{3N2} + \rho L_{N2}^2(s_{N2}\bar{s}_{N2}\ddot{q}_{N2} - c_{N2}\bar{c}_{N2}\ddot{\bar{q}}_{N2}) + \rho v^2 s\varphi c\theta - F_1 s\varphi s\theta + F_2 c\varphi = 0 \quad (21)$$

where k_{iN2} $(i = 1, 2, 3)$ are as in Eqs. (10–12) for $n = N2$ and $s\varphi \hat{=} \sin\varphi$, $c\varphi \hat{=} \cos\varphi$, $s\theta \hat{=} \sin\theta$, and $c\theta \hat{=} \cos\theta$. The angles φ and θ, appearing in Fig. 2b, can be accurately defined as

$$\varphi \hat{=} \tan^{-1}\left.\frac{\mathrm{d}z}{\mathrm{d}x}\right|_{\boldsymbol{x}=\boldsymbol{p}^{N2}\cdot\boldsymbol{n}_1}, \qquad \theta \hat{=} \tan^{-1}\left.\frac{\mathrm{d}y}{\mathrm{d}x}\cos\varphi\right|_{\boldsymbol{x}=\boldsymbol{p}^{N2}\cdot\boldsymbol{n}_1} \quad (22)$$

if TP is described by $y = f(x)$ and $z = g(x)$. Equations (19–21) comprise three equations with four unknowns $\ddot{q}_{N2}$, $\ddot{\bar{q}}_{N2}$, F_1, and F_2. An additional equation is obtained in conjunction with Eqs. (1), which must be satisfied throughout the motion, as follows: $\boldsymbol{v}^{P_{N2}} \cdot \boldsymbol{n}_{pi}$ $(i = 1, 2)$ are differentiated with respect to time and expressed as in Eqs. (A8) and (A9) in the Appendix with the aid of $\boldsymbol{n}_{p1}$ and $\boldsymbol{n}_{p2}$, given by

$$\boldsymbol{n}_{p1} = -s\theta c\varphi\boldsymbol{n}_1 + c\theta\boldsymbol{n}_2 - s\theta s\varphi\boldsymbol{n}_3, \qquad \boldsymbol{n}_{p2} = -s\varphi\boldsymbol{n}_1 + c\varphi\boldsymbol{n}_3 \quad (23)$$

(see Fig. 2a). The requisite equations are obtained if the right-hand sides of Eqs. (A8) and (A9) are set equal to zero, namely,

$$\boldsymbol{a}^{P_{N2}} \cdot \boldsymbol{n}_{p1} - v_1^{P_{N2}}\dot{\theta}/c\theta c\varphi = 0 \quad (24)$$

$$\boldsymbol{a}^{P_{N2}} \cdot \boldsymbol{n}_{p2} - v_1^{P_{N2}}\dot{\varphi}/c\varphi = 0 \quad (25)$$

in agreement with Eqs. (1), where $\boldsymbol{a}^{P_{N2}}$ is obtained from Eqs. (5), written for $n = N2$. Now one can solve Eqs. (19–21) and (25) [the role of Eq. (24) will become apparent shortly] for $\ddot{q}_{n2}$, $\ddot{\bar{q}}_{n2}$, F_1, and F_2. With

$$X \hat{=} s\theta c_{N2}\bar{c} - c\theta s_{N2}, \qquad Y \hat{=} c\theta c_{N2}\bar{c} + s\theta s_{N2}$$

$$Z \hat{=} -a_1^{P_{N2-1}}s\varphi + a_3^{P_{N2-1}}c\varphi - v_1^{P_{N2-1}}c\varphi\dot{\varphi} - v_3^{P_{N2-1}}s\varphi\dot{\varphi} + L_{N2}c_{N2}\bar{s}\left(\dot{q}_{N2}^2 + \dot{\bar{q}}_{N2}^2\right) - 2L_{N2}s_{N2}\bar{c}\dot{q}_{N2}\dot{\bar{q}}_{N2} \quad (26)$$

one arrives at the following expressions:

$$F_1 = \frac{c_{N2}(k_{1N2}c\varphi\bar{c} + k_{2N2}t_{N2} + k_{3N2}s\varphi\bar{c} + \rho L_{N2}\bar{s}Z) + \rho v^2 Y}{X} \quad (27)$$

$$F_2 = k_{1N2}s\varphi - k_{3N2}c\varphi - \rho L_{N2}Z \quad (28)$$

$$\ddot{q}_{N2} = \frac{k_{2N2} + F_1 c\theta + \rho v^2 s\theta}{\rho L_{N2}^2 c_{N2}} \quad (29)$$

$$\ddot{\bar{q}}_{N2} = \frac{\rho v^2 s\varphi c\theta - F_1 s\varphi s\theta + F_2 c\varphi + k_{3N2}}{\rho L_{N2}^2 c_{N2}\bar{c}_{N2} + t_{N2}\bar{t}_{N2}\ddot{q}_{N2}} \quad (30)$$

where

$$\bar{s} \hat{=} \sin(\varphi - \bar{q}_{N2}), \qquad \bar{c} \hat{=} \cos(\varphi - \bar{q}_{N2}) \quad (31)$$

and where $\dot{\varphi}$ is given by Eq. (A6). Thus, if A_{N1-1} is known, then, in the context of numerical integration, $\ddot{q}_{N1}, \ldots, \ddot{q}_{N2}$, $\ddot{\bar{q}}_{N1}, \ldots, \ddot{\bar{q}}_{N2}$, F_1, and F_2 can be determined with a repeated use of Eqs. (10–12), (16–18), and Eq. (6), for $n = N1, \ldots, N2 - 1$, along with Eqs. (10–12) and (27–30) for $n = N2$, provided $q_{N1}, \ldots, q_{N2}$, $\bar{q}_{N1}, \ldots, \bar{q}_{N2}$, $\dot{q}_{N1}, \ldots, \dot{q}_{N2}, \dot{\bar{q}}_{N1}, \ldots, \dot{\bar{q}}_{N2}$, $\boldsymbol{v}^P$, $\boldsymbol{v}^C$, and $\boldsymbol{a}^C$ (where $\boldsymbol{a}^{P_{N1-1}} = \boldsymbol{a}^C$) are known. In other words, if A_{N1-1} is given, then $\ddot{q}_{N1}, \ldots, \ddot{q}_{N2}, \ddot{\bar{q}}_{N1}, \ldots, \ddot{\bar{q}}_{N2}, F_1$, and F_2 can be determined with one pass of the indicated equations. One may conclude that the values of $\ddot{q}_{N1}, \ldots, \ddot{q}_{N2}, \ddot{\bar{q}}_{N1}, \ldots, \ddot{\bar{q}}_{N2}, F_1$, and F_2 depend on A_{N1-1}, as yet an unknown quantity. Hence, the following question must be addressed: What is the value of A_{N1-1} satisfying Eq. (24)? [Note that Eq. (25) has been used to construct Eqs. (27–30).] A novel approach to this question is based on the following observation, namely, that $\ddot{q}_{N1}, \ldots, \ddot{q}_{N2}, \ddot{\bar{q}}_{N1}, \ldots, \ddot{\bar{q}}_{N2}, F_1$, and F_2 depend

linearly on A_{N1-1}. Equations (10–12), (16–18), and (6) indicate that A_n $(n = N1, \ldots, N2-1)$, $\ddot{q}_n$ $(n = N1, \ldots, N2-1)$, and $\ddot{\bar{q}}_n$ $(n = N1, \ldots, N2-1)$ depend linearly on A_{n-1} and hence on $A_{n-2}, A_{n-3}, \ldots$, etc.; and similar dependence of $\ddot{q}_{N2}$, $\ddot{\bar{q}}_{N2}$, F_1, and F_2 on A_{n-1} is indicated by Eqs. (10–12) (for $n = N2$) and Eqs. (27–30). Moreover, $\boldsymbol{v}^{P_{N2}} \cdot \boldsymbol{n}_{p1}$ and $\boldsymbol{v}^{P_{N2}} \cdot \boldsymbol{n}_{p2}$ comprise linear combinations of $\dot{q}_{N1}, \ldots, \dot{q}_{N2}$ and $\dot{\bar{q}}_{N1}, \ldots, \dot{\bar{q}}_{N2}$. Accordingly, one can define a function D as

$$D \hat{=} \frac{\mathrm{d}}{\mathrm{d}t}\left(\boldsymbol{v}^{P_n} \cdot \boldsymbol{n}_{p1}\right) = \sum_{r=N1}^{N2} C_r \ddot{q}_r + \sum_{r=N1}^{N2} \bar{C}_r \ddot{\bar{q}}_r + E \tag{32}$$

where C_r $(r = N1, \ldots, N2)$ and $\bar{C}_r$ $(r = N1, \ldots, N2)$ are functions of $q_{N1}, \ldots, q_{N2}, \bar{q}_{N1}, \ldots, \bar{q}_{N2}$, and time t, and E is a function of $q_{N1}, \ldots, q_{N2}, \bar{q}_{N1}, \ldots, \bar{q}_{N2}, \dot{q}_{N1}, \ldots, \dot{q}_{N2}, \dot{\bar{q}}_{N1}, \ldots, \dot{\bar{q}}_{N2}$, and t; and one can conclude that D is a linear function of $\ddot{q}_{N1}, \ldots, \ddot{q}_{N2}$ and $\ddot{\bar{q}}_{N1}, \ldots, \ddot{\bar{q}}_{N2}$ and hence of A_{N1-1}. In view of Eq. (24), this function equals zero, that is,

$$D = \alpha A_{N1-1} + \beta = 0 \tag{33}$$

where α is a function of $q_{N1}, \ldots, q_{N2}, \bar{q}_{N1}, \ldots, \bar{q}_{N2}$, and t, and β is a function of $q_{N1}, \ldots, q_{N2}, \bar{q}_{N1}, \ldots, \bar{q}_{N2}, \dot{q}_{N1}, \ldots, \dot{q}_{N2}, \dot{\bar{q}}_{N1}, \ldots, \dot{\bar{q}}_{N2}$, and t. The question regarding A_{N1-1} can thus be replaced with the following one: What is the value of A_{N1-1} satisfying Eq. (33)? A three-pass procedure can be used to answer this question. Accordingly, D is evaluated for two guesses of A_{N1-1}, say A'_{N1-1} and A''_{N1-1}, i.e.,

$$D(A'_{N1-1}) = \alpha A'_{N1-1} + \beta \tag{34}$$

$$D(A''_{N1-1}) = \alpha A''_{N1-1} + \beta \tag{35}$$

and, because $D = 0$ [Eq. (33)],

$$A_{N1-1} = -\frac{\beta}{\alpha} = \frac{A'_{N1-1} D(A''_{N1-1}) - A''_{N1-1} D(A'_{N1-1})}{D(A''_{N1-1}) - D(A'_{N1-1})} \tag{36}$$

Consequently, two passes are required to determine A_{N1-1}, and one additional pass is required to determine the associated $\ddot{q}_{N1}, \ldots, \ddot{q}_{N2}, \ddot{\bar{q}}_{N1}, \ldots, \ddot{\bar{q}}_{N2}$, F_1, and F_2, provided that $q_{N1}(t), \ldots, q_{N2}(t)$, $\bar{q}_{N1}(t), \ldots, \bar{q}_{N2}(t), \dot{q}_{N1}(t), \ldots, \dot{q}_{N2}(t)$, and $\dot{\bar{q}}_{N1}(t), \ldots, \dot{\bar{q}}_{N2}(t)$ satisfy Eqs. (1).

B. Release of Links from *P*

When the distance between P_{N2} and $\bar{P}$ reaches the value L_{N2+1}, say, at time t_{N2+1}, then the $(N2+1)$th link is released. At that time q_{N2+1} and $\bar{q}_{N2+1}$ are introduced, having the values

$$\bar{q}_{N2+1}(t_{N2+1}) = \tan^{-1} \Delta z / \Delta x|_{t=t_{N2+1}} \tag{37}$$

$$q_{N2+1}(t_{N2+1}) = \tan^{-1} \Delta y / (\Delta x^2 + \Delta z^2)^{\frac{1}{2}}\Big|_{t=t_{N2+1}} \tag{38}$$

where Δx, Δy, and Δz are defined as follows. Let $\boldsymbol{r}^{\bar{P}}$ and $\boldsymbol{p}^{P_{N2}}$ be the position vectors of $\bar{P}$ and of P_{N2}, respectively, relative to a point fixed in $\mathfrak{n}$. Then

$$\Delta x \hat{=} (\boldsymbol{r}^{\bar{P}} - \boldsymbol{p}^{P_{N2}}) \cdot \boldsymbol{n}_1, \qquad \Delta y \hat{=} (\boldsymbol{r}^{\bar{P}} - \boldsymbol{p}^{P_{N2}}) \cdot \boldsymbol{n}_2$$
$$\Delta z \hat{=} (\boldsymbol{r}^{\bar{P}} - \boldsymbol{p}^{P_{N2}}) \cdot \boldsymbol{n}_3 \tag{39}$$

Similarly, $\dot{q}_{N2+1}$ and $\dot{\bar{q}}_{N2+1}$ are introduced at t_{N2+1}. For that purpose, consider $\bar{P}_{N2+1}$ and P_{N2+1}, the endpoints of C_{N2+1}, coinciding, respectively, with P_{N2} and $\bar{P}$ so that

$$\boldsymbol{v}^{\bar{P}_{N2+1}}(t \geq t_{N2+1}) = \boldsymbol{v}^{P_{N2}}$$
$$\boldsymbol{v}^{P_{N2+1}}(t \geq t_{N2+1}) = \boldsymbol{v}^{P_{N2}} + \omega^{C_{N2+1}} \times \boldsymbol{r}^{P_{N2}/P_{N2+1}} \tag{40}$$

Here, $\boldsymbol{r}^{P_{N2}/P_{N2+1}}$ is the position vector from P_{N2} to P_{N2+1}, and $\omega^{C_{N2+1}}$ is the angular velocity of C_{N2+1} in $\mathfrak{n}$, given by

$$\omega^{C_{N2+1}} = -\bar{s}_{N2+1}\dot{q}_{N2+1}\boldsymbol{n}_1 - \dot{\bar{q}}_{N2+1}\boldsymbol{n}_2 + \bar{c}_{N2+1}\dot{q}_{N2+1}\boldsymbol{n}_3 \tag{41}$$

Furthermore, the constraints described by Eqs. (1) are removed from P_{N2}, and the constraints $\boldsymbol{v}^{P_{N2+1}} \cdot \boldsymbol{n}_{pi}$ $(t > t_{N2+1}) = 0$ $(i = 1, 2)$ are imposed on P_{N2+1}, where now $\boldsymbol{n}_{pi}$ $(i = 1, 2)$ are perpendicular to TP at P_{N2+1}. Dot multiplying Eq. (40) with $\boldsymbol{n}_{pi}$ $(i = 1, 2)$ [see Eqs. (23)] throughout, one obtains two equations that, when solved for $\dot{q}_{N2+1}(t_{N2+1})$ and $\dot{\bar{q}}_{N2+1}(t_{N2+1})$, result in

$$\dot{q}_{N2+1}(t_{N2+1}) = \frac{v_1^{P_{N2}} s\theta \bar{c}_{N2+1} - v_2^{P_{N2}} c\theta \bar{c} + v_3^{P_{N2}} s\theta \bar{s}_{N2+1}}{L_{N2+1}(s\theta s_{N2+1} + c\theta c_{N2+1}\bar{c})} \tag{42}$$

$$\dot{\bar{q}}_{N2+1}(t_{N2+1}) = \frac{v_1^{P_{N2}} s\varphi + v_3^{P_{N2}} c\varphi - L_{N2+1}\bar{s}s_{N2+1}\dot{q}_{N2+1}(t_{N2+1})}{L_{N2+1}c_{N2+1}\bar{c}} \tag{43}$$

Next, suppose C_{N2+1} moves with one endpoint attached to P_{N2} and another sliding along TP before t_{N2+1}. Then both $\boldsymbol{v}^{P_{N2+1}}(t_{N2+1} - \varepsilon)$ and $\boldsymbol{v}^{P_{N2+1}}(t_{N2+1} + \varepsilon)$, where ε is an infinitely small time quantity, are given by the right-hand side of Eq. (40). That is, $\boldsymbol{v}^{P_{N2+1}}(t_{N2+1} + \varepsilon) = \boldsymbol{v}^{P_{N2+1}}(t_{N2+1} - \varepsilon)$, and, consequently, $\boldsymbol{v}^{P_n}(t_{N2+1} + \varepsilon) = \boldsymbol{v}^{P_n}(t_{N2+1} - \varepsilon)$ $(n = N1, \ldots, N2)$. It follows that $\dot{q}_n(t_{N2+1} + \varepsilon) = \dot{q}_n(t_{N2+1} - \varepsilon)$ and $\dot{\bar{q}}_n(t_{N2+1} + \varepsilon) = \dot{\bar{q}}_n(t_{N2+1} - \varepsilon)$ $(n = N1, \ldots, N2+1)$, and that, therefore, the release of an additional link from P is free of impulses.[16]

Finally, $N2+1$ is renamed $N2$. This procedure resembles that used in Ref. 5.

C. Release of Links from *C*

Let T_{N1-1} be the tension at $\bar{P}_{N1}$, given by

$$T_{N1-1} = \frac{A_{N1-1}}{c_{N1}\bar{c}_{N1}} \tag{44}$$

If $T_{N1-1} \leq \bar{T}$, then the length of C_{N1} remains L_{N1}, and $\boldsymbol{v}^{P_{N1}} = \boldsymbol{v}^{\hat{C}} + \omega^{N1} \times L_{N1}\boldsymbol{c}_{1N1}$, or

$$\boldsymbol{v}^{P_{N1}} = \boldsymbol{v}^{\hat{C}} - (\dot{\bar{q}}_{N1}\boldsymbol{n}_2 - \dot{q}_{N1}\boldsymbol{c}_{3N1}) \times L_{N1}\boldsymbol{c}_{1N1} \tag{45}$$

where $\boldsymbol{c}_{iN1}$ $(i = 1, 2, 3)$ play the role of $\boldsymbol{c}_{in}$ $(i = 1, 2, 3)$ in Fig. 2a for $n = N1$. However, when T_{N1-1} first exceeds $\bar{T}$, then the length of C_{N1}, now denoted L, is allowed to increase, while $\bar{P}_{N1}$, still in contact with $\hat{C}$, is acted upon by a force

$$\boldsymbol{F}^{\bar{P}_{N1}} = -\bar{T}\boldsymbol{c}_{1N1} \tag{46}$$

Under these circumstances, Eq. (45) gives way to

$$\boldsymbol{v}^{P_{N1}} = \boldsymbol{v}^{\hat{C}} - (\dot{\bar{q}}_{N1}\boldsymbol{n}_2 - \dot{q}_{N1}\boldsymbol{c}_{3N1}) \times L\boldsymbol{c}_{1N1} + \dot{L}\boldsymbol{c}_{1N1} \tag{47}$$

and the acceleration of P_{N1} becomes

$$\begin{aligned}\boldsymbol{a}^{P_{N1}} = \boldsymbol{a}^{\hat{C}} &- \left[L\left(\dot{q}_{N1}^2 + c_{N1}^2\dot{\bar{q}}_{N1}^2\right) - \ddot{L}\right]\boldsymbol{c}_{1N1} \\ &+ \left[L\left(\ddot{q}_{N1} + s_{N1}c_{N1}\dot{\bar{q}}_{N1}^2\right) + 2\dot{q}_{N1}\dot{L}\right]\boldsymbol{c}_{2N1} \\ &- [L(2s_{N1}\dot{q}_{N1}\dot{\bar{q}}_{N1} - c_{N1}\ddot{\bar{q}}_{N1}) - 2c_{N1}\dot{\bar{q}}_{N1}\dot{L}]\boldsymbol{c}_{3N1}\end{aligned} \tag{48}$$

If k_{1N1}, k_{2N1}, and k_{3N1} are defined:

$$\begin{aligned}k_{1N1} \hat{=} &-\bar{T}c_{N1}\bar{c}_{N1} - \rho L\left[a_1^{\hat{C}} - Lc_{N1}\bar{c}_{N1}\left(\dot{q}_{N1}^2 + \dot{\bar{q}}_{N1}^2\right)\right. \\ &+ 2Ls_{N1}\bar{s}_{N1}\dot{q}_{N1}\dot{\bar{q}}_{N1} - 2(c_{N1}\bar{s}_{N1}\dot{\bar{q}}_{N1} + \bar{c}_{N1}s_{N1}\dot{q}_{N1})\dot{L} \\ &\left. + c_{N1}\bar{c}_{N1}\ddot{L}\right] + D_1^{P_{N1}}\end{aligned} \tag{49}$$

$$\begin{aligned}k_{2N1} \hat{=} &-\bar{T}s_{N1} - \rho L\left(a_2^{\hat{C}} - Ls_{N1}\dot{q}_{N1}^2\right. \\ &\left. + 2c_{N1}\dot{q}_{N1}\dot{L} + s_{N1}\ddot{L}\right) + D_2^{P_{N1}}\end{aligned} \tag{50}$$

$$\begin{aligned}k_{3N1} \hat{=} &-\bar{T}c_{N1}\bar{s}_{N1} - \rho L\left[a_3^{\hat{C}} - Lc_{N1}\bar{s}_{N1}\left(\dot{q}_{N1}^2 + \dot{\bar{q}}_{N1}^2\right)\right. \\ &- 2Ls_{N1}\bar{c}_{N1}\dot{q}_{N1}\dot{\bar{q}}_{N1} - 2(s_{N1}\bar{s}_{N1}\dot{q}_{N1} \\ &\left. - c_{N1}\bar{c}_{N1}\dot{\bar{q}}_{N1})\dot{L} + c_{N1}\bar{s}_{N1}\ddot{L}\right] + D_3^{P_{N1}}\end{aligned} \tag{51}$$

then Eqs. (13–15) with $n = N1$ govern the motion of C_{N1}, with L replacing L_n. Moreover, Eqs. (16–18) remain valid for $n = N1$ with L replacing L_n. However, $\dot{L}$ replaces A_{N1-1} as an unknown, and the previous linear dependence of A_n ($n = N1, \ldots, N2-1$), $\ddot{q}_n$ ($n = N1, \ldots, N2$), $\ddot{\bar{q}}_n$ ($n = N1, \ldots, N2$), F_1, and F_2 on A_{N1-1} is replaced by a linear dependence of these variables on $\ddot{L}$. Consequently, $\ddot{L}$ replaces A_{N1-1} as the unknown in Eq. (33), and precisely the same three-pass procedure previously used to identify A_{N1-1} can be used here to identify $\ddot{L}$, the respective guesses being $\ddot{L}'$ and $\ddot{L}''$. Thus,

$$\ddot{L} = -\frac{\beta}{\alpha} = \frac{\ddot{L}'D(\ddot{L}'') - \ddot{L}''D(\ddot{L}')}{D(\ddot{L}'') - D(\ddot{L}')} \tag{52}$$

provided $\dot{L} > 0$. When $\dot{L}$ first becomes negative, say at t_L, Eq. (36) and the associated procedure regain validity, with $L(t_L)$, now a constant, replacing L_{N1}.

Release of an additional link from C occurs when L reaches the value $L_{N1} + L_{N1-1}$, say at time t_{N1-1}. Then q_{N1-1}, $\bar{q}_{N1-1}$, $\dot{q}_{N1-1}$, and $\dot{\bar{q}}_{N1-1}$ are introduced as follows:

$$q_{N1-1}(t_{N1-1}) = q_{N1}(t_{N1-1}) \tag{53}$$

$$\bar{q}_{N1-1}(t_{N1-1}) = \bar{q}_{N1}(t_{N1-1}) \tag{54}$$

$$\dot{q}_{N1-1}(t_{N1-1}) = \dot{q}_{N1}(t_{N1-1}) \tag{55}$$

$$\dot{\bar{q}}_{N1-1}(t_{N1-1}) = \dot{\bar{q}}_{N1}(t_{N1-1}) \tag{56}$$

Now consider points $\bar{P}_{N1-1}$ and P_{N1-1}, the endpoints of C_{N1-1}, the former coinciding with $\hat{C}$ and the latter located a distance L_{N1-1} from $\bar{P}_{N1-1}$ along C_{N1}. With $\omega^{C_{N1-1}}$ and $\omega^{C_{N1}}$ as the angular velocities of C_{N1-1} and C_{N1} in $\mathcal{N}$, one has

$$\boldsymbol{v}^{\bar{P}_{N1-1}} = \boldsymbol{v}^{\hat{C}} \tag{57}$$

$$\omega^{C_{N1-1}} = \omega^{C_{N1}} = -\dot{\bar{q}}_{N1}\boldsymbol{n}_2 + \dot{q}_{N1}\boldsymbol{c}_{3N1} \tag{58}$$

and

$$\boldsymbol{v}^{P_{N1-1}}(t_{N1-1}) = \boldsymbol{v}^{\hat{C}} + \omega^{C_{N1-1}} \times L_{N1-1}\boldsymbol{c}_{1N1} + \dot{L}\boldsymbol{c}_{1N1} \tag{59}$$

Suppose C_{N1-1} moves with one endpoint attached to $\hat{C}$ and another lying along C_{N1} before t_{N1-1}. Then both $\boldsymbol{v}^{P_{N1-1}}(t_{N1-1} - \varepsilon)$ and $\boldsymbol{v}^{P_{N1-1}}(t_{N1-1} + \varepsilon)$ are given by the right-hand side of Eq. (59). That is, $\boldsymbol{v}^{P_{N1-1}}(t_{N1-1}+\varepsilon) = \boldsymbol{v}^{P_{N1-1}}(t_{N1-1}-\varepsilon)$, and, consequently, $\boldsymbol{v}^{P_n}(t_{N1-1}+\varepsilon) = \boldsymbol{v}^{P_n}(t_{N1-1}-\varepsilon)$ ($n = N1, \ldots, N2$). It follows that $\dot{q}_n(t_{N1-1}+\varepsilon) = \dot{q}_n(t_{N1-1}-\varepsilon)$ and $\dot{\bar{q}}_n(t_{N1-1}+\varepsilon) = \dot{\bar{q}}_n(t_{N1-1}-\varepsilon)$ $n = N1-1, \ldots, N2$) and that, therefore, the release of an additional link from C is free of impulses.[16]

Finally, $N1 - 1$ is renamed $N1$.

D. Initial Conditions and Simulations

The following initial conditions have been chosen, namely, $N2(0) = N1(0)$, so that $N(0) = 1$, and

$$\bar{q}_{N2}(0) = \tan^{-1}(z^{\bar{P}} - z^{\hat{C}})/(x^{\bar{P}} - x^{\hat{C}})|_{t=0} \tag{60}$$

$$q_{N2}(0) = \tan^{-1}(y^{\bar{P}} - y^{\hat{C}}) \Big/ \left[(x^{\bar{P}} - x^{\hat{C}})\bar{c}_{N2}(0)\right]\Big|_{t=0} \tag{61}$$

where $x^{\hat{C}}$, $y^{\hat{C}}$, and $z^{\hat{C}}$ are the Cartesian coordinates of $\hat{C}$, and where it is implied that the distance from $\bar{P}$ to $\hat{C}$ equals, at $t = 0$, L_{N2}. Furthermore,

$$\dot{q}_{N2}(0) = \frac{v_1^{\hat{C}} s\theta\bar{c}_{N2} - v_2^{\hat{C}} c\theta\bar{c} + v_3^{\hat{C}} s\theta\bar{s}_{N2}}{L_{N2}(s\theta s_{N2} + c\theta c_{N2}\bar{c})} \tag{62}$$

$$\dot{\bar{q}}_{N2}(0) = \frac{v_1^{\hat{C}} s\varphi + v_3^{\hat{C}} c\varphi - L_{N2}\bar{s}s_{N2}\dot{q}_{N2}(0)}{L_{N2}c_{N2}\bar{c}} \tag{63}$$

where $v_i^{\hat{C}}$ ($i = 1, 2, 3$) are the $\boldsymbol{n}_i$ ($i = 1, 2, 3$) measure numbers of $\boldsymbol{v}^{\hat{C}}$. Equations (62) and (63) are obtained if Eq. (4), written for $n = N2(0)$, is dot multipled by $\boldsymbol{n}_{pi}$ ($i = 1, 2$) [see Eqs. (23)], substituted in Eqs. (1), and solved for $\dot{q}_{N2}(0)$ and $\dot{\bar{q}}_{N2}(0)$.

Thus, all of the ingredients required to simulate the motion of the cable are in hand.

Figures 3 and 4 are obtained with a cable of $\rho = 2.8\ 10^{-4}$ kg/m. The trajectory TP is given by $y = 35\sin(x\pi/350)$ m and $z = 7\sin(x\pi/350)$ m, and $v_i^{\bar{P}} = \dot{x} = 100tu(1-t) + 100u(t-1)$ m/s [where $u(\ )$ is the unit step function]. The trajectory TC is given by $x = 30(\cos\alpha - 1)$ m, $y = 30\sin\alpha$ m, $z = -4t$ m, and $v_3^{\hat{C}} = 30\dot{\alpha}\cos\alpha$ m/s, where $\dot{\alpha} = 0.5\pi tu(2-t) + \pi(2-t/2)\ u(t-2)$ rad/s. That part of the cable contained in V_C is 60 m long. The deployed cable is subject to gravity, to a back wind of 20 m/s in the $\boldsymbol{n}_1$ direction, and to a side wind of 20 m/s in the $\boldsymbol{n}_3$ direction (the associated aerodynamic model is not reported here but can be found, e.g., in Ref. 17). Snapshots of the cable at $t = 1.2$ and 4 s for $\bar{T} = 4N$ are shown in Fig. 3. The intermittent line and the dotted line designate TP and TC, respectively. The heavy line and the light line indicate parts of the cable deployed from V_C, consisting at $t = 4$ s of 60 1-m-long links, and from V_P, consisting at $t = 4$ s of 50 1-m-long links and of 62 4-m-long links, respectively [this means that at $t = 4$ s the problem becomes one of $2(60 + 50 + 62) - 1 = 343$ degrees of freedom]. Finally, the stars and the circles indicate the locations of $\bar{P}$ and of $\hat{C}$, respectively. Figure 4 shows the tension $T_{N1-1}(= A_{N1-1}/c_{N1}\bar{c}_{N1})$ at $\bar{P}_{N1}$ for $\bar{T} = 4N$ (thin line) and for $\bar{T} = 40N$ (intermittent line). With $\bar{T} = 40N$ no links are released from V_C, and the cable assumes a configuration similar to that with $\bar{T} = 4N$, except in regions where T_{N1-1} exceeds $4N$. Moreover, with $\bar{T} = 4N$, the last of the 60 links of C is deployed at $t = 2.8$ s, an event giving rise to an instantaneous increase in the cable tension. Additional runs show that, in fact, termination of deployment from V_C causes the tension at $\hat{C}$ to reach the value it would have achieved with no cable deployment from V_C, as when $\bar{T} = 40N$. Figure 4 indicates that if the permissible tensile strength of the cable is $15N$, then no deployment from $\hat{C}$ and, consequently, no force control mechanism are needed. On the other hand, if the permissible tensile strength of the cable is only $4N$, then one has to set $\bar{T} = 4N$. Additional runs show that, in this event, the minimal number of 1-m-long links in V_C with which a tension of $4N$ will not be exceeded throughout the motion is 77 (all of which will have been deployed by $t = 4$ s). Finally, figures similar to Figs. 3 (top) and 4 are obtained if TP and TC are replaced by their planar projection and if no side wind is present. In that event, $\bar{q}_n \equiv 0 (n = N1, \ldots, N2)$, $\dot{\bar{q}}_n \equiv 0$ ($n = N1, \ldots, N2$), $\theta \equiv 0$, and $\dot{\theta} \equiv 0$.

Discussion

A few points associated with the new algorithm deserve elaboration.

1) The left-hand side of Eq. (24) was used as D in Eq. (33). By the same token, any of the left-hand sides of Eqs. (19–21), (24), and (25) can play the role of D.

2) Disconnection of the cable from $\bar{P}$ starting, say at $t = t_{\bar{P}}$, can be incorporated in the simulation. Then the constraints [Eqs. (1)] are removed, and Eqs. (20) and (21) are solved for $\ddot{q}_{N2}$ and $\ddot{\bar{q}}_{N2}$ with $F_1 = F_2 = 0$. These, replacing Eqs. (27–30), together with D in Eq. (33), which is now defined as the left-hand side of Eq. (19), are implemented in the simulation code.

3) Disconnection of the cable from $\hat{C}$ starting, say at $t = t_{\hat{C}}$, can be incorporated in the simulation. This can be achieved if, for $t > t_{\hat{C}}$, L is allowed to increase indefinitely with $\bar{T} = 0$.

4) The lengths of the links can be chosen at will, so that shorter links can be used to capture regions of small radii of curvature.

5) Knowledge of the tension acting in each of the links [see Eq. (16)] enables the evaluation of the deployment reliability (a matter of interest when the deployment of an optical fiber is under investigation).

6) The algorithm can be easily modified so as to take into account such factors as the elastic properties of the cable, the moments of inertia of the links, etc. For example, suppose $\boldsymbol{T}_{n-1}$ and $\boldsymbol{T}_n$ are torques of elastic couples exerted by C_{n-1} on C_n and by C_n on C_{n+1}, respectively, and that $T_{n-1}^{(i)}$ and $T_n^{(i)}$ ($i = 1, 2, 3$) are the respective measure numbers in the $\boldsymbol{n}_i$ ($i = 1, 2, 3$) directions. Then Eqs. (7) and (8) are replaced with

$$A_{n-1}^{(2)} = A_{n-1}t_n \Big/ \bar{c}_n + \left[T_{n-1}^{(3)} - T_n^{(3)}\right] \Big/ L_n c_n \bar{c}_n$$

$$A_{n-1}^{(3)} = A_{n-1}\bar{t}_n - \left[T_{n-1}^{(2)} - T_n^{(2)}\right] \Big/ L_n c_n \bar{c}_n$$

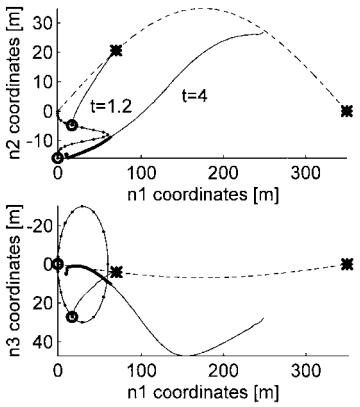

Fig. 6 Snapshots of cable configurations; disconnection from P and C at $t = 3$ s.

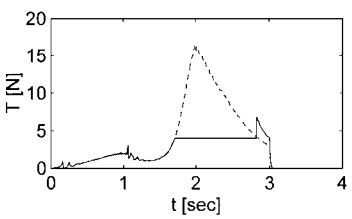

Fig. 7 Cable tension at $\hat{C}$; disconnection from P and C at $t = 3$ s.

Eqs. (10–12) are redefined accordingly, and the rest of the algorithm remains unaltered. Note that $T_{n-1}^{(i)}$ and $T_n^{(i)}$ $(i = 1, 2, 3)$ can be expressed in terms of the bending rigidity of the cable and of q_{n-1}, $\bar{q}_{n-1}$, q_n, $\bar{q}_n$, q_{n+1}, and $\bar{q}_{n+1}$. Material damping can be accounted for similarly.

7) A numerical solution of the constraint equations in Ref. 6 gives rise to constraint violation, alleviated with the aid of Baumgarte's constraint stabilization procedure. Here, the three-pass procedure, in conjunction with a Kutta–Merson variable step integrator, does not give rise to constraint violation even when the number of links becomes large (172 in the example).

8) A wide range of cable-associated problems, involving either a constant or a variable length cable, can be solved with minor modifications of the present algorithm. For example, one can disconnect $\bar{P}$ from the cable (see comment 2) and attribute inertial properties to C_{N2} (see comment 6). One then obtains cable deployment from C only, with a rigid body attached to the cable at P_{N2-1}. One can, furthermore, abandon the assumption that $\boldsymbol{v}^{\hat{C}}$ is prescribed and, alternatively, obtain $\boldsymbol{v}^{\hat{C}}$, solving 12 differential equations governing an unconstrained motion of C, while C is subject to a force $\boldsymbol{T}$ at $\hat{C}$. Finally, one can let $\boldsymbol{T}$ be a control force, designed to optimize the deployment process.

Results of the implementation of comments 2 and 3 are illustrated in Figs. 6 and 7, where $t_{\bar{P}} = t_{\hat{C}} = 3$ s. The cable is swept away while P and C carry on with their missions, which, under the specified wind conditions, bear no risk of interference of P and C with the floating cable. The tension at $\hat{C}$ drops to zero at $t = 3$ s, as might be expected.

Conclusion

A new algorithm is presented, underlying the simulation of the deployment of a cable from two independently moving platforms. It differs from earlier works in that it regards the cable as a dynamical system consisting of a time-dependent number of links, subject to a deployment-monitoring sequence of constraints removal and imposition; it introduces a novel, three-pass procedure for the identification of constraint forces and of second time derivatives of integration variables; and it can be modified easily so as to deal with a wide range of systems of the type in question.

Appendix: Kinematic Relationships for P_{N2}

Point term P_{N2} moves along TP, and if x, y, and z are the coordinates of P_{N2} in $\mathfrak{n}$, then, in view of Eqs. (16),

$$\dot{x} = v_1^{P_{N2}}, \qquad \dot{y} = v_2^{P_{N2}}, \qquad \dot{z} = v_3^{P_{N2}} \tag{A1}$$

$$\frac{\dot{y}}{\dot{x}} = \frac{v_2^{P_{N2}}}{v_1^{P_{N2}}} = \frac{\tan\theta}{c\varphi} \tag{A2}$$

$$\frac{\dot{z}}{\dot{x}} = \frac{v_3^{P_{N2}}}{v_1^{P_{N2}}} = \tan\varphi \tag{A3}$$

$$\boldsymbol{v}^{P_{N2}} = v_1^{P_{N2}}(\boldsymbol{n}_1 + \tan\theta/c\varphi\boldsymbol{n}_2 + \tan\varphi\boldsymbol{n}_3) \tag{A4}$$

[see Eqs. (59) and (60)]. Moreover, $\tan\theta = (\mathrm{d}y/\mathrm{d}x)c\varphi$ and $\tan\varphi = \mathrm{d}z/\mathrm{d}x$, so that

$$\dot{\theta} = c^2\theta c\varphi(y'' - y'z''s\varphi c\varphi)v_1^{P_{N2}} \tag{A5}$$

$$\dot{\varphi} = c^2\varphi z'' v_1^{P_{N2}} \tag{A6}$$

Noting that ω, the angular velocity of a reference frame fixed to $\boldsymbol{n}_t$, $\boldsymbol{n}_{p1}$, and $\boldsymbol{n}_{p2}$, is given by

$$\omega = -s\varphi\dot{\theta}\boldsymbol{n}_1 - \dot{\varphi}\boldsymbol{n}_2 + c\varphi\dot{\theta}\boldsymbol{n}_3 \tag{A7}$$

one has, using Eqs. (A4), (A7), and (23),

$$\frac{\mathrm{d}\left(\boldsymbol{v}^{P_{N2}} \cdot \boldsymbol{n}_{p1}\right)}{\mathrm{d}t} = \boldsymbol{a}^{P_{N2}} \cdot \boldsymbol{n}_{p1} + \boldsymbol{v}^{P_{N2}} \cdot \omega \times \boldsymbol{n}_{p1}$$
$$= \boldsymbol{a}^{P_{N2}} \cdot \boldsymbol{n}_{p1} - v_1^{P_{N2}}\dot{\theta}/c\theta c\varphi \tag{A8}$$

$$\frac{\mathrm{d}\left(\boldsymbol{v}^{P_{N2}} \cdot \boldsymbol{n}_{p2}\right)}{\mathrm{d}t} = \boldsymbol{a}^{P_{N2}} \cdot \boldsymbol{n}_{p2} + \boldsymbol{v}^{P_{N2}} \cdot \omega \times \boldsymbol{n}_{p2}$$
$$= \boldsymbol{a}^{P_{N2}} \cdot \boldsymbol{n}_{p2} - v_1^{P_{N2}}\dot{\varphi}/c\varphi \tag{A9}$$

References

[1]Misra, A. K., and Modi, V. J., "A General Dynamical Model for the Space Shuttle Based Tether Satellite System," *Advances in the Astronautical Sciences*, Vol. 40, Pt. 2, 1979, pp. 537–557.

[2]Liangdong, L., and Bainum, P. M., "Effects of Tether Flexibility on the Tethered Shuttle Subsatellite Stability and Control," *Journal of Guidance, Control, and Dynamics*, Vol. 12, No. 6, 1989, pp. 866–873.

[3]Djerassi, S., "Dynamics of a Satellite Retracting a Long Elastic Appendage," *Journal of the Astronautical Sciences*, Vol. 44, No. 4, 1997, pp. 425–442.

[4]Keshmiri, M., Misra, A. K., and Modi, V. J., "General Formulation for N-Body Tethered Satellite System Dynamics," *Journal of Guidance, Control, and Dynamics*, Vol. 19, No 1, 1996, pp. 75–83.

[5]Banerjee, A. K., "Order-n Formulation of Extrusion of a Beam with Large Bending and Rotation," *Journal of Guidance, Control, and Dynamics*, Vol. 15, No. 1, 1990, pp. 121–127.

[6]Banerjee, A. K., and Do, V. N., "Deployment Control of a Cable Connecting a Ship to an Underwater Vehicle," *Journal of Guidance, Control, and Dynamics*, Vol. 17, No. 6, 1994, pp. 1327–1332.

[7]Kamman, J. W., and Huston, R. L., "Modeling of Submerged Cables Dynamics," *Computer and Structures*, Vol. 20, No. 1–3, 1985, pp. 623–629.

[8]Cochran, J. E., Innocenti, M., No, T. S., and Thukral, A., "Dynamics and Control of Maneuverable Towed Flight Vehicles," *Journal of Guidance, Control, and Dynamics*, Vol. 15, No. 5, 1992, pp. 1245–1252.

[9]Clifton, J. M., Schmidt, L. V., and Stuart, T. D., "Dynamic Modeling of a Trailing Wire Towed by an Orbiting Aircraft," *Journal of Guidance, Control, and Dynamics*, Vol. 18, No. 4, 1995, pp. 875–881.

[10]Loeser, H. T., and Doebler, H. J., "Tactical Expendable Device," U.S. Patent No. 4,473,896, Sept. 25, 1984.

[11]Pinson, G. T., "Communication Link Between Moving Bodies," U.S. Patent No. 4,860,968, Aug. 29, 1989.

[12]Holzschuh, J. F., and Hightower, D., "Towed Fiber Optic Data Link Payout System," U.S. Patent No. 5,419,512, May 30, 1995.

[13]Hughes, P. C., and Sincarsin, G. B., "Dynamics of an Elastic Multibody Chain, Parts A and B," *Dynamics and Stability of Systems*, Vol. 4, Nos. 3 and 4, 1989, pp. 209–226, 227–244.

[14]Bae, D. S., and Hauge, E. J., "A Recursive Formulation for Constrained Mechanical Systems: Part I, Open Loop Systems," *Mechanics of Structures and Machines*, Vol. 15, No. 3, 1987, pp. 359–382.

[15]Rosenthal, D., "An Order-n Formulation for Robotic Systems," *Journal of the Astronautical Sciences*, Vol. 38, No. 4, 1998, pp. 511–529.

[16]Djerassi, S., "Imposition of Constraints," *Journal of Applied Mechanics*, Vol. 61, No. 2, 1994, pp. 434–439.

[17]Dekel, E., and Pnueli, D., "Simulation of a Thin Wire Deployed from an Aircraft," *Proceedings of the 34th Israel Annual Conference of Aerospace Sciences*, Haifa, Israel, 1994, pp. 73–78.